J. Electrochem. Sci. Eng. **13(1)** (2023) 137-147; http://dx.doi.org/10.5599/jese.1316

Open Access : : ISSN 1847-9286

www.jESE-online.org

Original scientific paper

Microhardness and biological behavior of AZ91D-nHAp surface composite for bio-implants

Satpal Kundu and Lalit Thakur✉

[1]*Mechanical Engineering Department, NIT Kurukshetra, Haryana, Pincode-136119, India*

Corresponding author: ✉lalitthakur@nitkkr.ac.in

Received: March 3, 2022; Accepted: April 6, 2022; Published: May 18, 2022

Abstract

In the present research work, friction stir processing (FSP) has been adopted for the fabrication of nano-hydroxyapatite (nHAP) reinforced AZ91-D Mg-alloy matrix surface composite (NMMSC). The NMMSC was developed to replace the conventional bio-implants materials for short-term usage. The NMMSC has been prepared by adding nHAp reinforcement in 12.5 % volumetric proportion in the AZ91-D alloy using the grooving technique followed by FSP. The FSP parameters were selected, such as the tool rotation of 1000 rpm, 50 mm/min transverse speed, and 5 multi-passes. The base alloy, normal FSPed, and fabricated NMMSC were characterized to study their micro-hardness values and biological performances. Improvement in microhardness value in the developed composites was observed due to the smaller grain size as a result of the dynamic recrystallization phenomenon. The antibacterial properties of FSPed and NMMSC specimens tested against Staphylococcus aureus, Candida albicans, and Aspergillus fumigatus were found to be superior as compared to the PM. The cytotoxicity of the FSPed & NMMSC specimens expressed as cell viability using MTT assay shows negligible toxicity as compared to PM and the cell viability was insignificantly decreased as the incubation period was extended. The microhardness and biological performance of NMMSC have been improved due to the grain refinement by FSP and the presence of nHAp reinforcement in the material.

Keywords

Magnesium AZ91D; nano-hydroxyapatite; nano metal matrix surface composite; friction stir processing

Introduction

Magnesium and its alloys are one of the growing research areas for short-term bio-implant materials, particularly for loadbearing orthopedic applications. In the case of implant replacement, biodegradable magnesium avoids follow-up surgery after the tissue is healed [1]. Due to its good mechanical properties and load-bearing capacity, magnesium is selected for biomaterial application. With magnesium and its alloys, the stress shielding effect can be minimized due to its elastic modulus, density, and yield strength being nearer to the human bone material as

compared to other bio-implant materials [2-4]. On the other hand, pure Mg has a higher rate of corrosion in the physiological environment, which leads to the release of hydrogen [5,6]. The implant may fail in loadbearing conditions due to a lack of good mechanical properties [7]. Many surface treatments have been performed to stop the degradation by changing the composition and microstructure, such as using the protective layers and alloying [5,6,8-11]. Selecting the appropriate reinforcement and its volume % in the manufacturing of metal matrix composite (MMC) using Mg as a matrix for biomedical areas is beneficial because the biological and mechanical characteristics can be improved. In the case of fine grained Mg alloys for bio-implants applications, an improvement in the mechanical, corrosion, and biological properties has been reported [12-15]. Among the alloys of Mg in the AZ series, AZ91-D is a very common alloy due to its good castability, corrosion resistance, and better mechanical properties [16]. AZ91D indicates that the proportions of aluminium and zinc are about 9 and 1 (% weight), respectively and the remaining amount is balanced by Mg. The presence of aluminum in the alloy improves its cast-ability and also increases its hardness and tensile strength up to a temperature of 120 °C [17].

Nano-hydroxyapatite (nHAp) is a calcium phosphate mineral similar to the mineral of natural bone. It is known to be a bio-ceramic material due to its excellent bioactivity, biocompatibility, and ability to bind with the bones [16]. In the biological fluids, the top layer of the Mg-nHAp composites has exhibited a similar crystallographic and chemical structure as the bone with an appropriate second phase due to the distribution of Ca-P compounds [18]. In bio-implants, the synthesised nHAp has proven to be quite effective at preventing infection [19]. Moreover, it has been reported that corrosion behavior and mechanical properties are enhanced because of the dispersion of nHAp in the composite [18].

Friction stir processing (FSP) is a well-known technique of surfacē engineering which is used for the surface modification and processing of surface composites. The grain refinement was found to be enhanced because of the dispersion of HAp particles in Mg alloy by using FSP [15]. In the FSP technique, the process of grain refinement has been reported [20,21]. Here, a cylindrical hard rotating tool with a pin is plunged into the material surface being processed and is traversed along the desired length, which causes the dynamic recrystallization in the material because of severe plastic deformation produced inside the stirring zone [21]. This causes grain refinement in the processed material. The distribution of the secondary phase and particles during the grain refinement is also observed is due to the stirring action of the tool, which improves the surface properties of the material. Firstly, Mishra [20] successfully manufacture the composite of Al with reinforcement of SiC using FSP. Considerable work has been reported on performing the MMSC using Al and Mg as the matrix or reinforcement of oxides and carbides using the characterization of microstructure, hardness, and wear properties [22-27]. The studies on the fabrication of bio-ceramic reinforced Magnesium alloy surface composites for bio-implants using the FSP are limited. Therefore, in this research article, a small attempt has been made to develop the nHAp reinforced AZ91D Mg alloy matrix surface composite (NMMC) for bio-implants using the FSP technique. The comparative study of microstructure, mechanical, antibacterial behavior, and cytotoxicity of parent AZ91D material, friction stir processed (FSPed), and NMMSC specimens have been conducted in the present research work.

(cc) BY

Experimental

Composite fabrication

In this research article, 150×100×6 mm sheets of AZ91D Mg alloy were taken as the parent matrix material (PM) and finished to remove any geometrical deformities and surface oxides. Thereafter, a groove of 2 mm in depth and 1.5 mm in width was machined on the surface of sheets with the help of a shaper machine to keep the 12.5 % nHAp reinforcement volumetric concentration. nHAp reinforcement powder was filled properly in this groove with the help of injection thoroughly and then it was packed by ramming the surface with a wooden mallet. Sealing of reinforcement-filled grooves was done by a pin-less FSP tool, as shown in Figure 1. Finally, the FSP was carried out on the sealed grooves using a threaded profile pin-type tool made of HS-13 material having a shoulder of 17 mm diameter, pin diameter of 5.7 mm, pin length 3.1 mm length, and a tilt angle was kept constant to 1°. The friction stir process parameters were used as the tool rotation of 1000 rpm, 50 mm/min transverse speed, and 5 number of multi-passes, respectively.

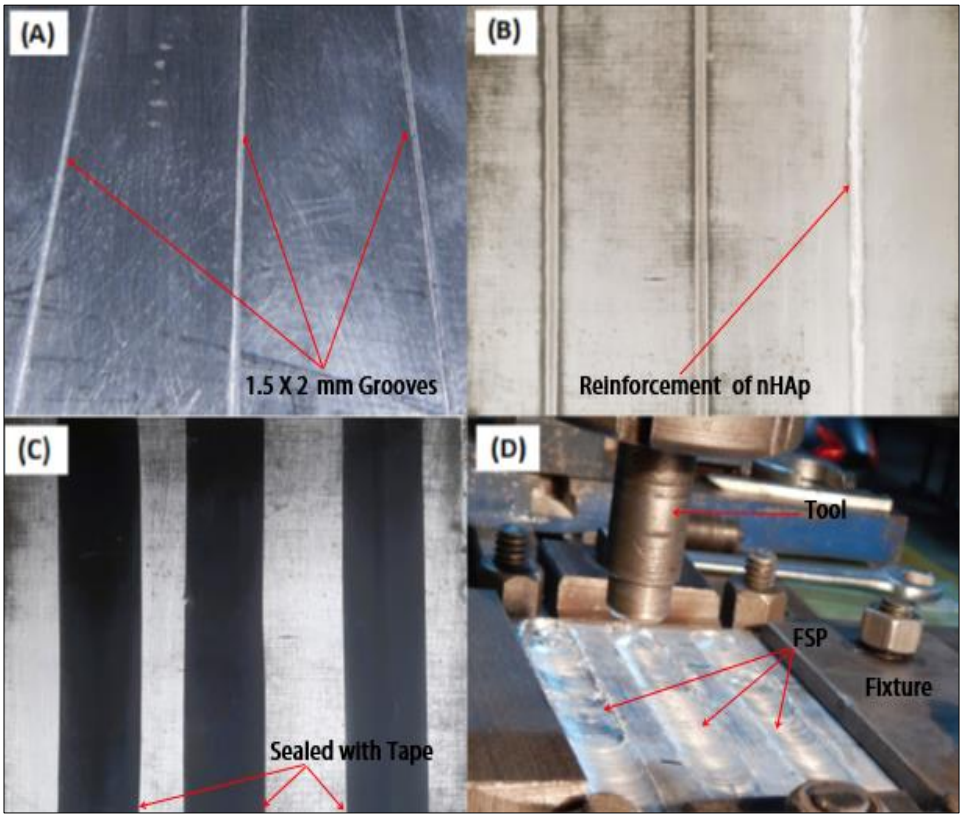

Figure 1. *FSP followed by (a) cutting grooves, (b) added nHAp reinforcement, (c) sealing of filled grooves, (d) friction stir processing*

Microstructural and microhardness study

The compositional and microstructural examination was performed by using an energy-dispersive X-ray spectroscope coupled with a scanning electron microscope (SEM), JSM-6390 LV, Jeol Japan. Moreover, a metallurgical microscope (Suxma Moto, Conation Technologies Pune, India) of 1000× magnification was used to analyze the grains of the specimens. The metallographic samples were cut perpendicular to the tool traverse direction and polished by using emery papers of different grades, followed by the electro-polishing method with a solution of 99 % ethanol and 1 % perchloric acid. X-ray diffraction (XRD) analysis was conducted on the specimens using an X-ray diffractometer (Bruker D8 advance) at a scanning speed of 1°/min and a scan range of 20-90°, respectively.

Microhardness testing was conducted on the specimens using a microhardness tester (XHVT-1000Z, Jinan testing equipment, China). The micro-indents were taken over the cross-section of specimens by the application 100 g load with a 10 sec dwell time. The indents were taken out on the FSPed regions (at the cross-sections and top surface). Micro-hardness was calculated on the cross-section of the specimens. In the case of the FSPed and composite specimens, it was evaluated along with the depth and width of the stir zone, respectively.

The antibacterial activity

The biological performance of the PM, FSPed, and NMMSC was assessed through the antibacterial activity of these specimens with human pathogenic microorganism strains such as Staphylococcus aureus, Escherichia coli, and Candida albicans using Laminar Air Flow Apparatus. Triplicate plates were developed for each specimen of size 4 × 5 × 6 mm, prepared from the intermediate portion of the PM and stir zones of the FSPed and NMMSC samples. The microorganisms taken in this investigation were preferred due to their clinical significance. *Escherichia coli* and *Staphylococcus aureus* were cultivated at 37 ^{o}C in nutrient agar (NA), using peptone 5 g/L, beef extract 3 g/L, agar 20 g/L, and NaCl 5 g/L, respectively. Candida albicans was cultivated on potato-dextrose-agar (PDA) with the medium compositions (M3): 4 g/L potato infusion, 15 g/L agar, and 20 g/L dextroses; also, a temperature of 4 °C was kept for the culture of the stock. The Clinical Laboratory of National Committee Standards conducted the inhibition zone evaluation test [28]. A sterile medium of 20 mL was placed into a Petri dish and 1 mL of the microbial strain was disseminated on agar plates, and sterile samples were placed on the plate surface. To allow microbiological development, all tests were cultivated for bacterial activity at 37 °C for 24 h and at 28 °C for 48 h yeast. The ability of the sample to halt bacterial multiplication around it was considered to evaluate its antibacterial activity.

Cytotoxicity

MTT [3(4,5-181 dimethyl-thiazole 2yl)2, 5 diphenyl tetrazolium bromide] was exposed to the skeletal muscle cells of rats (procured from the National Centre for Cell Sciences Pune, India) for 72 hours to calculate the cytotoxicity of the samples [29]. All samples were put in the plate of 96-well culture, with 100 µl of cell solution holding 10^5 cells planted in each well. The samples with cell-seeded cultures were analyzed for 24, 48, and 72 h at 37 °C in a humidified environment with 5 % CO_2. Each well received 150 µl of culture media. A 20 µl MTT solution was added to each well, followed by a 4 h incubation at 37 °C. The samples were incubated with dimethyl sulfoxide, and with reference at 650 nm was used to measure the absorbance value and calculated at 570 nm microplate observer with non-seeded wells set. Each experiment was repeated three times and the average value of experiments was used.

The equation (1) was used to assess cell viability as a percentage of the control (standard polystyrene tissue culture plates).

Cell viability = (Mean optical density / Control optical density) 100 (1)

Results and discussion

Microstructural observations

Figure 2 represents the SEM image of the as-cast AZ91D magnesium alloy (PM) selected as the matrix material in the current study. The microstructure of PM shows the α-Mg grains arranged in different orientations and the presence of β-$Mg_{17}Al_{12}$ phase precipitated over the grain boundaries.

(cc) BY

EDX analysis has been performed to confirm the composition of the material's composition as claimed by the manufacturer, as shown in Figure 3 [30]. Figure 4 shows the SEM image of the nano-HAp reinforcement powder particles. These agglomerated particles exhibited a smooth spherical morphology in a size range of 15-45 µm. Moreover, tiny nano-HAp particles of about 20 nm size can be seen adhering to the surface of these agglomerated powder particles. Figure 5 shows the EDX analysis of nano-HAp powder feedstock material and it confirmed the presence of Ca and P as the major elements.

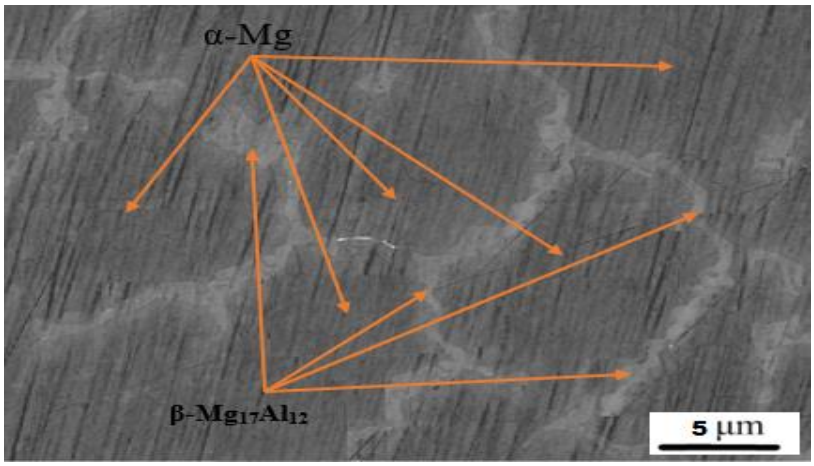

Figure 2. *SEM image of AZ91-D material*

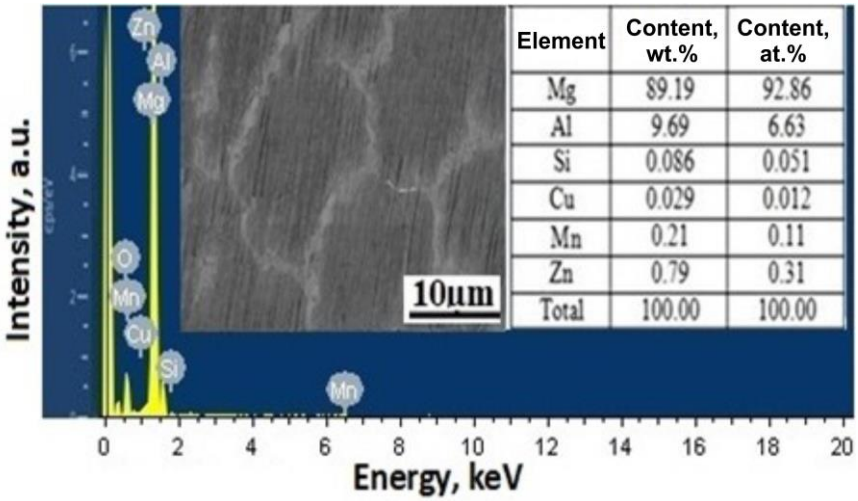

Element	Content, wt.%	Content, at.%
Mg	89.19	92.86
Al	9.69	6.63
Si	0.086	0.051
Cu	0.029	0.012
Mn	0.21	0.11
Zn	0.79	0.31
Total	100.00	100.00

Figure 3. *As cast AZ91-D material EDX analysis*

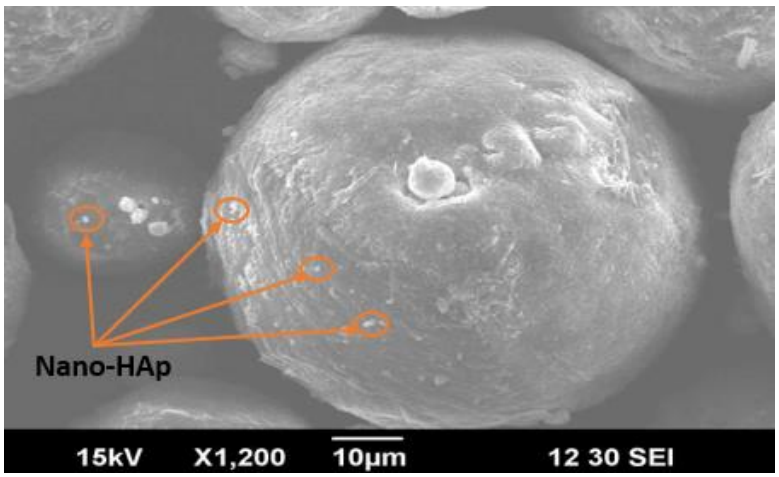

Figure 4. *SEM image of agglomerated nano-hydroxyapatite powder particles*

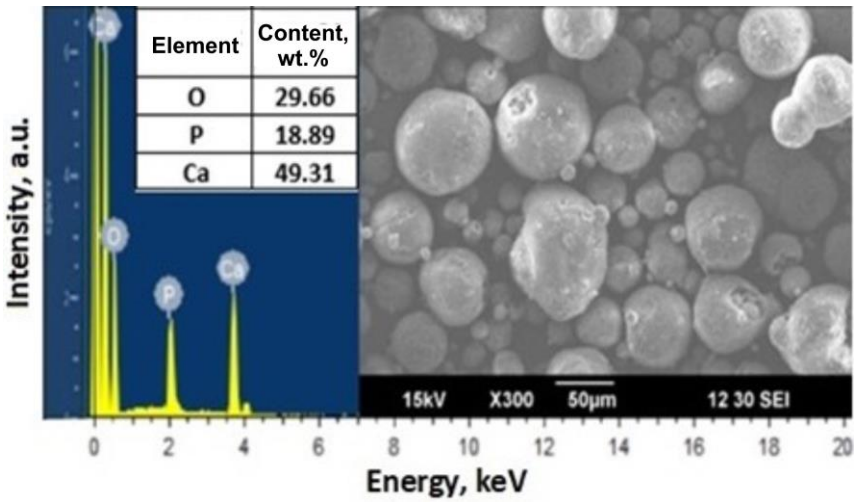

Figure 5. *EDX image of nano-HAp powder*

Figure 6 represents the optical microscopic (OM) cross-sectional images of the PM, FSPed, and NMMSCs specimens. The average grain size of PM was found to be 10.18 µm which was reduced to 2.14 µm in FSP, 1.82 µm in NMMSC specimens. The refined grain size confirmed that during the FSP, no melting of the AZ91D magnesium alloy occurred (*i.e.,* the temperature reached was lower than the melting point of magnesium, which was 650 °C) [23,26] and due to this Nano-HAp is stable in AZ91D matrix, Similar types of observations have been reported by Rameshbabu *et al.* [31]. X-ray diffraction (XRD) analyses and SEM combined with EDS have been carried out over PM, FSP, and NMMSC specimens, as represented in Figures 7 and 8, respectively. Due to the sufficient temperature increase, the friction and intense plastic deformation cause dynamic recrystallization, and also the initially present coarse β-phase in PM is broken into the fine size and dissolved into the matrix. The amount of β-phase in FSPed and NMMSC specimens has reduced, as seen from the XRD peaks. The images show that FSP has resulted in grain refinement because of the plastic flow of material inside the stir zone. Moreover, the presence of agglomerated nHAp has been fairly diffused and spread across the stir zone.

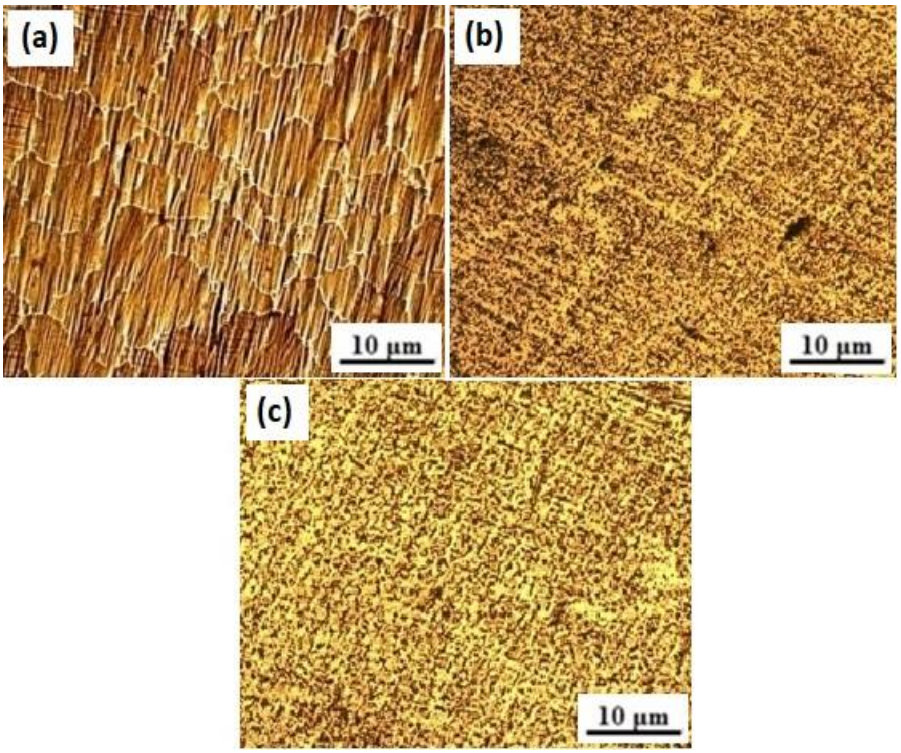

Figure 6. *OM images showing the microstructural features in (a) PM, (b) FSPed, and (c) NMMCs specimens*

CC BY

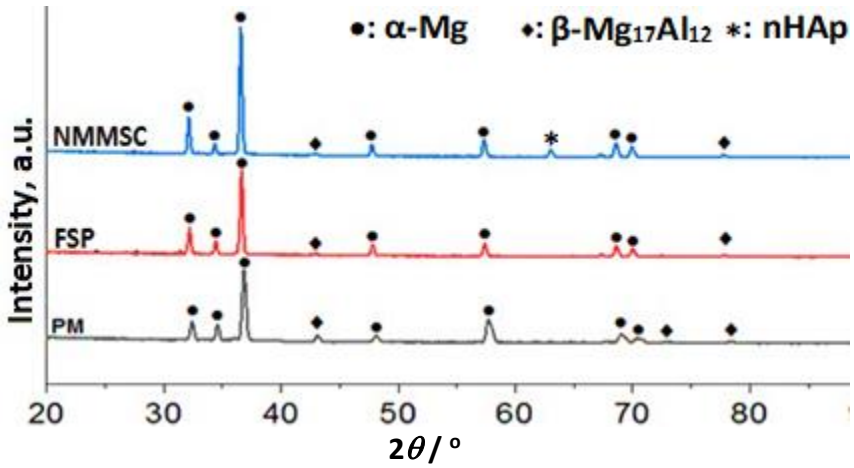

Figure 7. *XRD patterns observed in (a) PM, (b) FSPed, and (c) NMMC specimens*

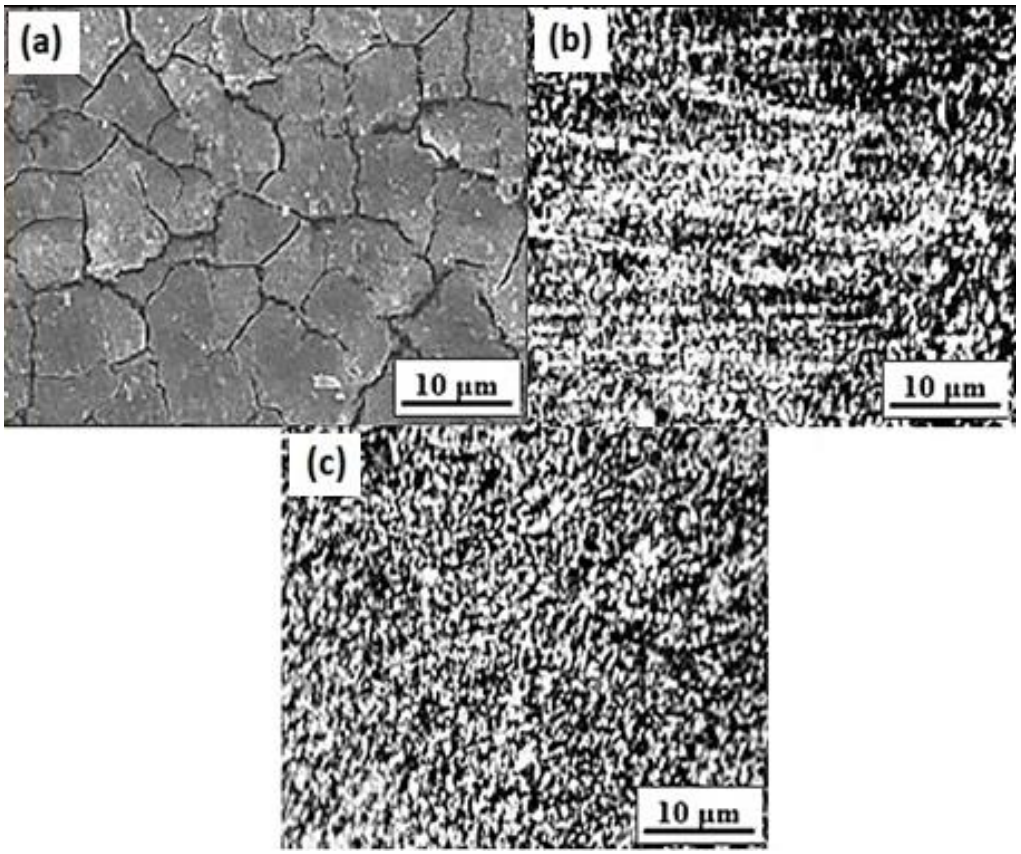

Figure 8. *SEM images representing microstructural features in (a) PM, (b) FSPed, and (c) NMMSC specimens*

Microhardness

The influence of hardness on grain growth of various specimens is visualized in Figure 9 by the microhardness distribution. The microhardness values varied significantly as well because most of NMMSCs and FSPed zones have a wide range of grain sizes. However, when compared to PM, the hardness over the surface of NMMSC and FSP was rather increased. The average microhardness values of the FSPed and NMMSC specimens along the depth of SZ were obtained as 83.8 HV, and 89.1 HV, and along the width of SZ were found to be 84.6 HV, and 92.3 HV, respectively. There is an acceptable difference in the microhardness of PM, FSPede, and NMMSC (along with the depth and width of the stir zone as shown in Figures 9. Samples of NMMSC and FSPed showed average hardness values at the lower portion of the cross-section and higher near the top surface when compared to PM in the stir zone because of the stimulating effect of thermal softening [32].

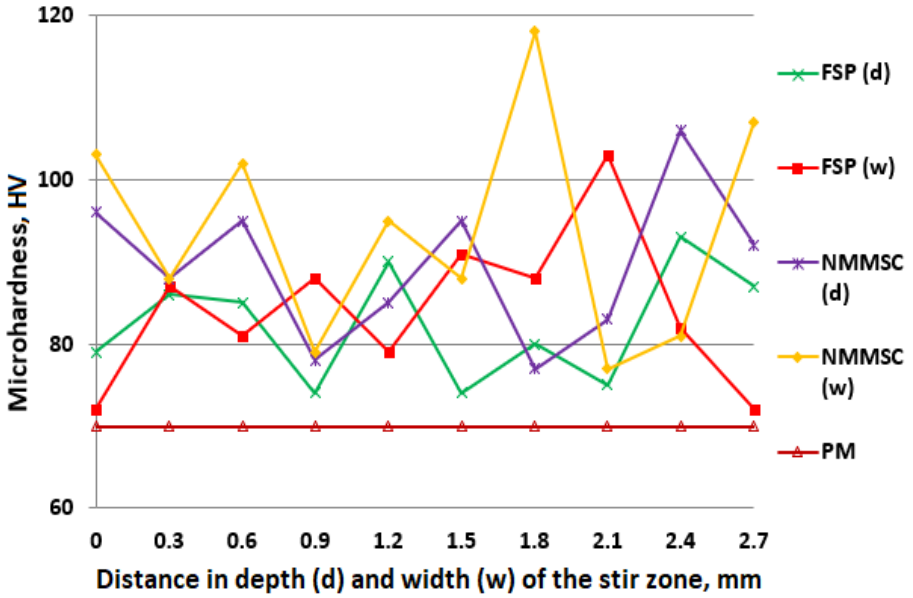

Figure 9. *Microhardness of PM, FSPed, and NMMSC specimens across distance in depth (d) and width (w) of the stir zone*

The antibacterial activity

Carotenoids generated by yeasts are crucial in resisting oxidative stress [11]. Oxidative stress occurs when the body's natural antioxidants and oxidizing species are out of balance and nHAp, as a carotenoid pigment, has strong antioxidant and antibacterial properties and can boost immunological function for a faster response to microbial threats. It can boost the expression of multiple genes linked to pathogen identification, and it could be a new approach in antibacterial behavior [8]. Nano-HAp was used as an antibacterial agent in this study. The comparison of bacterial activity of *Staphylococcus aureus* (Gram +Ve), *Escherichia coli* (Gram –Ve), and *Yeast-Candida Albicans* on the PM, FSPed, and NMMSC specimens is shown in Figure 10. It can be inferred that the pathogenic microbial strains' growth was found to be better in the NMMSC as compared to FSPed and PM specimens due to the presence of nano-HAp reinforcement in the material.

In this research, triplicate plates were produced for each specimen from the mid-region of the PM and stir zone of the FSPed and NMMSC and prepared specimens were examined for infectious microbial strains in humans such as *Staphylococcus aureus* (Gram +Ve), *Escherichia coli* (Gram –Ve) and *Yeast-Candida Albicans* are shown in Figure 11.

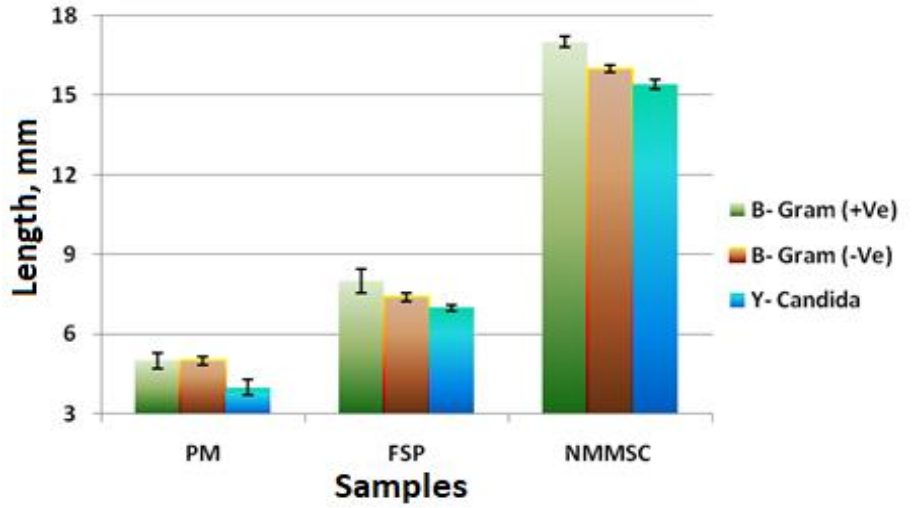

Figure 10. *Antibacterial activity of the specimens of PM, FSPed, and NMMSC*

(cc) BY

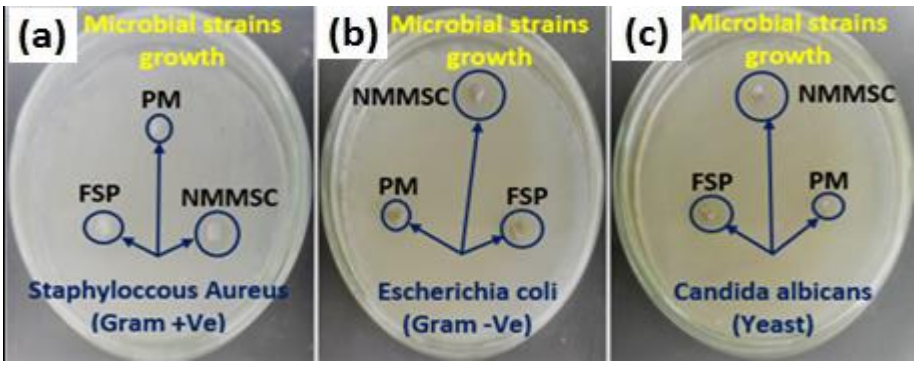

Figure 11. *Images showing the antibacterial activity of PM, FSPed, and NMMSC specimens (a) Staphylococcus aureus (Gram +Ve), (b) Escherichia coli (Gram –Ve), and (c) Yeast-Candida Albicans*

Cytotoxicity

The percentage viability related to the PM, FSPed, and NMMSC specimens against the L6 cells for 72 h is presented in Figure 12. Toxicity was found to be minimal in all the samples. As the incubation duration increases from 24 to 48 to 72 h, the cells show an equal response to all specimens. As the incubation time rise, the viability of PM and FSPed decreased slightly. In the case of NMMSC, there is no negative impact on the cell and It can be understood from the results that this is because of the small grain size and incorporated nHAp after processing. Embedded nHAp particle improves osseointegration [33] and reduces degradation rate, promoting cell adhesion [34]. The cells on the surface of PM were clustered and interconnected. On the other hand, the linked cells on the surfaces of the FSPed and NMMSC were observed to expand and attach to the surface. As seen in Figure 13, a large number of cells occupied the surface of the NMMSC and began to grow. Lower the degradation rate in NMMSC as compared to the other samples and enhance the osseointegration due to integrated nHAp particles.

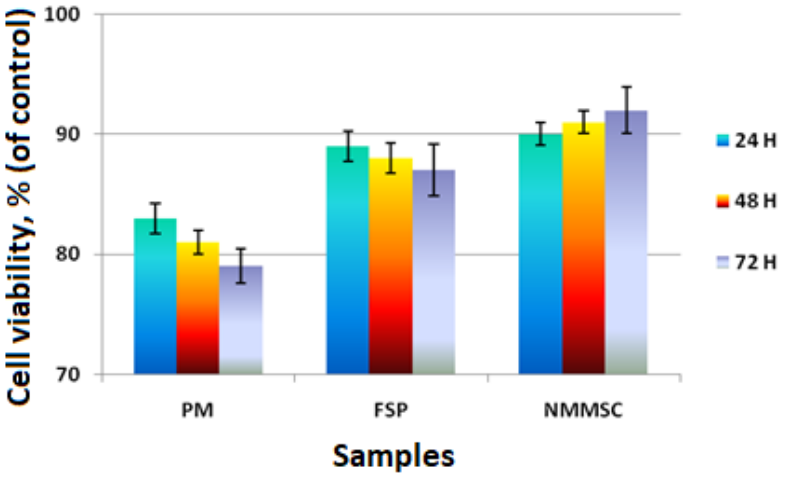

Figure 12. *Cytotoxicity of the samples of PM, FSPed, and NMMSC expressed as % cell viability using MTT assay*

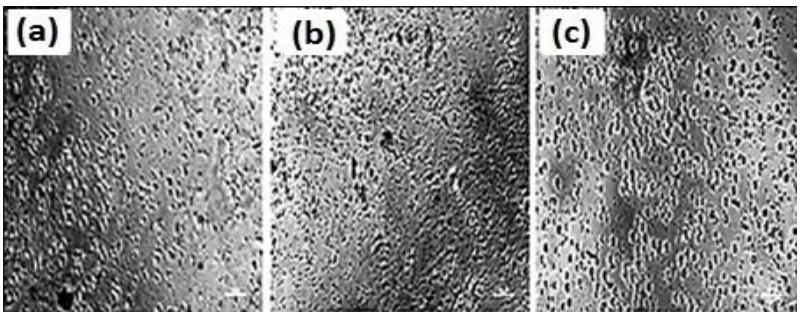

Figure 13. *Image showing the cytotoxicity activity of (a) PM, (b) FSPed, and (c) NMMSC specimens.*

Conclusion

In this research article, a comparative study was performed between PM, FSPed, and NMMSC specimens considering their microstructure, micro-hardness, antibacterial activity, and cytotoxicity as the main parameters. The observations demonstrated that the FSP has the potential method to introduce the nHAp reinforcement in different proportions in the AZ91D magnesium alloy to develop high-performance NMMSCs for bio-implants. The following conclusion can be made from the study:

- The maximum grain reduction was achieved in the case of NMMSC, followed by FSPed and PM specimens. Moreover, the pinning impact of reinforcements on the grain boundaries may be responsible for post grain growth inhibition in NMMSCs.
- The maximum microhardness was recorded in the case of NMMSC as compared to FSPed and PM. This was in agreement with the Hall-Petch equation of increased hardness as grain refinement.
- The ability of the PM, FSPed, and NMMSC specimens to halt bacterial growth around them was used to evaluate antimicrobial activity. The antibacterial properties allow microbial growth and also chemistry of the surface because the appearance of nano-hydroxyapatite affects the antibacterial activity.
- Cytotoxicity (as percentage viability) of FSPed and NMMSC specimens is more than the PM specimens. As the incubation time rise, each specimen demonstrated minimal toxicity and cells responded similarly to all of the samples.

References

[1] F. Witte, V. Kaese, H. Haferkamp, E. Switzer, A. M. Lindenberg, *Biomaterials* **26** (2005) 3557-3563. https://doi.org/10.1016/j.biomaterials.2004.09.049

[2] G. L. Song, *Corrosion Science* **49** (2007) 1696-1701. https://doi.org/10.1016/j.corsci.2007.01.001

[3] F. Witte, N. Hort, C. Vogt, S. Cohen, K. U. Kainer, R. Willumeit, F. Feyerabend, *Current Opinion in Solid State & Materials Science* **12** (2008) 63-72. https://doi.org/10.1016/j.cossms.2009.04.001

[4] F. Witte, J. Fischer, J. Nellesen, H.A. Crostack, V. Kaese, A. Pisch, F. Beckmann, H. Windhagen, *Biomaterials* **27** (2006) 1013-1018. https://doi.org/10.1016/j.biomaterials.2005.07.037

[5] H. Wang, Y. Estrin, Z. Zú berová, *Materials Letters* **62** (2008) 2476-2479. https://doi.org/10.1016/j.matlet.2007.12.052

[6] Y. Wang, M. Wei, J. Gao, J. Hu, Y. Zhang, *Materials Letters* **62** (2008) 2181-2184. https://doi.org/10.1016/j.matlet.2007.11.045

[7] X. Zhao, L.L. Shi, J. Xu, *Materials Science and Engineering C* **33** (2013) 3627-3637. https://doi.org/10.1016/j.msec.2013.04.051

[8] H. Hornberger, S. Virtanen, A.R. Boccaccini, *Acta Biomaterialia* **8** (2012) 2442-2455. https://doi.org/10.1016/j.actbio.2012.04.012

[9] S. Keim, J.G. Brunner, B. Fabry, S. Virtanen, *Journal of Biomedical Materials Research Part B: Applied Biomaterials* **96B** (2011) 84-90. https://doi.org/10.1002/jbm.b.31742

[10] T. S. N. Sankara Narayanan, I. S. Park, M. H. Lee, *Progress in Materials Science* **60** (2014) 1-71. https://doi.org/10.1016/j.pmatsci.2013.08.002

[11] S. Shaylin, J. D. George, *Acta Biomaterialia* **8** (2012) 20-30. https://doi.org/10.1016/j.actbio.2011. 10.016

[12] J. J. Martínez Sanmiguel, D. G. Zarate-Triviño, R. Hernandez-Delgadillo, A. L. Giraldo-Betancur, N. Pineda-Aguilar, S. A. Galindo-Rodríguez, M. A. Franco-Molina, S. P. Hernández-Martínez, C. Rodríguez-Padilla, *Journal of Biomaterials Applications* **33** (2019)1314-1326. https://doi.org/10.1177/0885328219835995

(cc) BY

[13] D. Franco, G. Calabrese, S. Petralia, G. Neri, C. Corsaro, L. Forte, S. Squarzoni, S. Guglielmino, F. Traina, E. Fazio, S. Conoci, *Molecules* **26** (2021) 1099. https://doi.org/10.3390/molecules26041099
[14] Q. Ge, D. Dellasega, A. G. Demir, M. Vedani, *Acta Biomaterialia* **9** (2013) 8604-8610. https://doi.org/10.1016/j.actbio.2013.01.010
[15] V. V. Ramalingam, P. Ramasamy, M. Govindaraju, S. Priyadharshini, *Materials Research Express* **6(8)** (2019) 085401. https://doi.org/10.1088/2053-1591/ab1ded
[16] W. Suchank, M. Yoshimura, *Journal of Materials Research* **13** (1998) 94-117. https://doi.org/10.1557/JMR.1998.0015
[17] R. S. Mishra, Z. Y. Ma, *Materials Science and Engineering* **50(1-2)** (2005) 1-78. https://doi.org/10.1016/j.mser.2005.07.001
[18] F. Witte, F. Feyerabend, P. Maier, J. Fischer, M. Stormer, C. Blawert, W. Dietzel, N. Hort, *Biomaterials* **28** (2007) 2163-2174. https://doi.org/10.1016/j.biomaterials.2006.12.027
[19] S. Lamkhao, M. Phaya, C. Jansakun, N. Chandet, K. Thongkorn, G. Rujijanagul, P. Bangrak, C. Randorn, *Scientific Reports* **9** (2019) 4015. https://doi.org/10.1038/s41598-019-40488-8
[20] R. S. Mishra, M. W. Mahoney, S. X. McFadden, N. A. Mara, A.K. Mukherjee, *Scripta Materialia* **42** (2000) 163-168. https://doi.org/10.1016/S1359-6462(99)00329-2
[21] R.S. Mishra, Z.Y. Ma, I. Charit, *Materials Science and Engineering A* **341** (2003) 307-310. https://doi.org/10.1016/S0921-5093(02)00199-5
[22] Y. Morisada, H. Fujii, T. Nagaoka, K. Nogi, M. Fukusumi, *Composites A* **38** (2007) 2097-2101. https://doi.org/10.1016/j.compositesa.2007.07.004
[23] W.B. Lee, C.Y. Lee, M.K. Kim, J.I. Yoon, Y.J. Kim, Y.M. Yoen, S.B. Jung, *Composite Science and Technology* **66** (2006) 1513-1520. https://doi.org/10.1016/j.compscitech.2005.11.023
[24] T.J. Chen, Z.M. Zhu, Y.D. Li, Y. Ma, Y. Hao, *Transactions of Nonferrous Metals Society of China* **20**(2010) 34-42. https://doi.org/10.1016/S1003-6326(09)60093-5
[25] C.J. Lee, J.C. Huang, P.J. Hsieh, *Scripta Materialia* **54** (2006) 1415-1420. https://doi.org/10.1016/j. scriptamat.2005.11.056
[26] M. Azizieh, A.H. Kokabi, P. Abachi, *Materials & Design* **32** (2011) 2034-2041. https://doi.org/10.1016/j. matdes.2010.11.055
[27] P. Asadi, G. Faraji, A. Masoumi, G.M. Besharati, *Metallurgical and Materials Transactions A* **42(9)** (2011) 2820-2832. https://doi.org/10.1007/s11661-011-0698-8
[28] M2-A9 Performance Standards for Antimicrobial Disk Susceptibility Tests, *Approved Standard* 9th edition*, Wayne, PA: CLSI* (2006).
[29] T. Mosmann, *Journal of Immunological Methods* **65** (1983) 55-63. https://doi.org/10.1016/0022-1759(83)90303-4
[30] R. Kumar, D. Bhandari, K. Goyal, *Journal of Electrochemical Science and Engineering* **12(4)** (2022) 651-666. http://dx.doi.org/10.5599/jese.1190
[31] N. Rameshbabu, K. Prasad Rao, T.S. Sampath Kumar, *Journal of Materials Science* **40** (2005) 6319-6323. https://doi.org/10.1007/s10853-005-2957-9
[32] R. S. Mishra, M. W. Mahoney, Friction stir welding and processing, *ASM International* (2007) 3-55. https://doi.org/10.1361/fswp2007p001
[33] H. Sakaki, T. Nakanishi, A. Tada, W. Miki, S. Komemushi, *Journal of Bioscience and Bioengineering* **92** (2001) 294-297. https://doi.org/10.1016/S1389-1723(01)80265-6
[34] J. B. Johnston, J. G. Nickerson, J. Daroszewski, T. J. Mogg, G. W. Burton, *PLoS One* **9** (2014) e111346. https://doi.org/10.1371/journal.pone.0111346

©2022 by the authors; licensee IAPC, Zagreb, Croatia. This article is an open-access article distributed under the terms and conditions of the Creative Commons Attribution license (https://creativecommons.org/licenses/by/4.0/)